PROCEEDINGS OF SPIE

SPIEDigitalLibrary.org/conference-proceedings-of-spie

Thermally insensitive determination of the chirp parameter of InAs/GaAs quantum dot lasers epitaxially grown onto silicon

J. Duan, H. Huang, B. Dong, D. Jung, Z. Zhang, et al.

J. Duan, H. Huang, B. Dong, D. Jung, Z. Zhang, J. C. Norman, J. E. Bowers, F. Grillot, "Thermally insensitive determination of the chirp parameter of InAs/GaAs quantum dot lasers epitaxially grown onto silicon," Proc. SPIE 10939, Novel In-Plane Semiconductor Lasers XVIII, 109390S (1 March 2019); doi: 10.1117/12.2509698

SPIE.

Event: SPIE OPTO, 2019, San Francisco, California, United States

Thermally insensitive determination of the chirp parameter of InAs/GaAs quantum dot lasers epitaxially grown onto silicon

J. Duan[a*], H. Huang[a], B. Dong[a], D. Jung[b], Z. Zhang[c], J. C. Norman[d], J. E. Bowers[b,c,d] and F. Grillot[a,e]
[a]LTCI, Télécom ParisTech, 46 Rue Barrault, 75013 Paris, France;
[b]Institute for Energy Efficiency, University of California Santa Barbara, Santa Barbara, California 93106, USA;
[c]Department of Electrical and Computer Engineering, University of California Santa Barbara, Santa Barbara, California 93106, USA;
[d]Materials Department, University of California Santa Barbara, Santa Barbara, California 93106, USA;
[e]Center for High Technology Materials, University of New-Mexico, 1313 Goddard SE, Albuquerque, NM 87106, USA
*jianan.duan@telecom-paristech.fr

ABSTRACT

A common way of extracting the chirp parameter (i.e., the α-factor) of semiconductor lasers is usually performed by extracting the net modal gain and the wavelength from the amplified spontaneous emission (ASE) spectrum. Although this method is straightforward, it remains sensitive to the thermal effects hence leading to a clear underestimation of the α-factor. In this work, we investigate the chirp parameter of InAs/GaAs quantum dot (QD) lasers epitaxially grown on silicon with a measurement technique evaluating the gain and wavelength changes of the suppressed side modes by optical injection locking. Given that the method is thermally insensitive, the presented results confirm our initial measurements conducted with the ASE i.e. the α-factor of the QD lasers directly grown on silicon is as low as 0.15 hence resulting from the low threading dislocation density and high material gain of the active region. These conclusions make such lasers very promising for future integrated photonics where narrow linewidth, feedback resistant and low-chirp on-chip transmitters are required.

Keywords: Quantum dots, Semiconductor lasers, Chirp parameter;

1. INTRODUCTION

Silicon photonics is a promising key enabling technology bringing multiple advantages to overcome the data transmission bottleneck of semiconductor microchips in terms of bandwidth limit and power density [1]. The integration of multiple optical functions on a microelectronics chip brings many innovative perspectives, along with the possibility to enhance the performance of photonics integrated circuits (PICs). Owing to the atom-like discrete energy levels, quantum dots (QDs) allow producing energy- and cost-efficient devices with outstanding properties such as low threshold current, good temperature stability and narrow linewidth [2,3]. In particular, direct epitaxial growth of GaAs layers onto silicon with InAs QDs as gain media has been proved to be a meaningful solution for inexpensive and monolithically integrated silicon light emitters [4,5]. In semiconductor lasers, the α-factor is a key parameter resulting from the phase-amplitude coupling effect, and driving the spectral linewidth [3], the sensitivity to optical feedback [6,7], the nonlinear dynamics under optical injection [8] and four-wave mixing generation [9]. The α-factor typically describes the coupling between the carrier-induced variation of real and imaginary parts of susceptibility and is defined as [10]:

$$\alpha = -\frac{4\pi}{\lambda}\frac{dn/dN}{dg/dN} \quad (1)$$

where *dn* and *dg* are the small refractive index and modal gain variations accompanied by a carrier density variation *dN* and λ is the lasing wavelength.

Novel In-Plane Semiconductor Lasers XVIII, edited by Alexey A. Belyanin, Peter M. Smowton, Proc. of SPIE Vol. 10939, 109390S · © 2019 SPIE
CCC code: 0277-786X/19/$18 · doi: 10.1117/12.2509698

At the system level, a large α-factor leads to a frequency chirp (Δν) under direct modulation, which is expressed as [11]:

$$\Delta\nu = -\frac{\alpha}{4\pi}\left(\frac{d}{dt}lnP + \frac{2\Gamma P\epsilon}{V_{act}\eta h\nu}\right) \quad (2)$$

where P is the optical power, Γ is the modal confinement factor, ϵ characterizes the gain compression factor, V_{act} is the active layer volume and η is the total differential quantum efficiency. The frequency chirp typically limits the maximum data rate and transmission distance over a dispersive fiber. Our recent work has previously reported α-factors as low as 0.13 in QD lasers directly grown onto silicon as a result of the low threading dislocation density [12]. The α-factors is usually measured from the standard amplified spontaneous emission (ASE) which relies on simultaneous observation of the longitudinal modes wavelength shift and the modal gain changes with varying current below lasing threshold [2]. However, due to residual thermal effects, the ASE measurement can possibly underestimate the α-factors. In order to confirm our initial measurements [12], this work investigates the α-factor with a thermally insensitive method based on the analysis of residual side-mode dynamics under optical injection. Such method has already been successfully tested in InAs/InP QD lasers [13]. Finally, results confirm that the α-factors initially measured in [12] are low with a minimum value of 0.15 at the gain peak. Given that the standard deviation does not exceeding 15%, we can conclude that both methods are found in a relative good agreement, which is obviously important when small values of the linewidth broadening factor are addressed. Overall, we believe that this work paves the way of future integrated optical transmitters on silicon with increased maximum transmission capabilities.

2. QD LASER STRUCTURE

The InAs/GaAs Fabry-Perot (FP) laser is 1.35 mm long with a 3.5 μm wide ridge waveguide directly grown onto an on-axis (001) Si wafer in a Veeco Gen-II molecular beam epitaxy chamber. The full laser epitaxial structure and QD growth conditions can be found elsewhere [14]. A schematic of the QD laser structure is presented in Figure 1. The p-modulation doped QD laser consists of 5 QD layers spaced by 37.5 nm thick GaAs barrier layers, where the first 10 nm GaAs layer was undoped, followed by a 10 nm p-GaAs layer at a target hole concentration of 5×10^{17} cm^{-3} using Be, and the final 17.5 nm GaAs layer was undoped again to complete the GaAs barrier. The QD density is 4.9×10^{10} cm^{-2} and the photoluminescence spectra of the full laser sample revealed a very small full-width at half-maximum (FWHM) of 29.3 meV from the ground

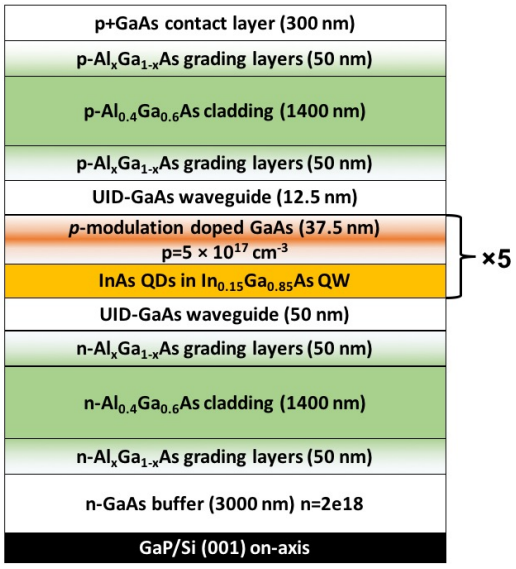

Figure 1. Cross-sectional schematic of an InAs QD laser epitaxially grown on (001) GaP/Si.

state (GS) peak (not shown), indicating a highly homogeneous InAs QD size throughout the 5 QD stacks. The front facet has a power reflectivity of ~60 % whereas a high reflectivity of ~99 % is used on the rear and the reduced threading dislocation

density (TDD) of 7.3 × 10^6 cm^{-2} in the active region has been achieved. At room temperature (20 ℃), the laser has a lasing threshold of 26.5 mA, and the GS gain peak was located around 1300 nm at 80 mA. The light-current characteristic curve is shown in Figure 2, where the marker in black corresponds to the bias current of 80 mA used to measure the optical spectrum depicted in the inset.

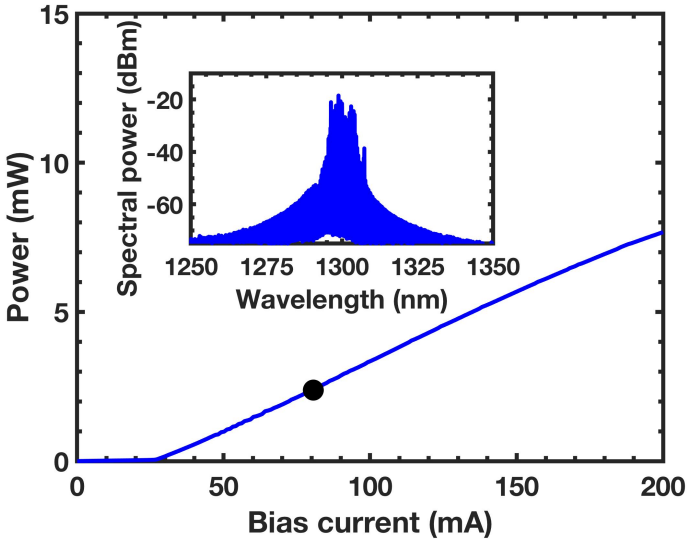

Figure 2. The light-current characteristic of the laser measured at room temperature (20 C°). The inset shows the optical spectrum at 80 mA (black marker).

3. EXPERIMENTAL SETUP AND RESULTS

In a prior work [12], the α-factor was initially measured by the ASE method, which relies on measuring the differential index by tracking the frequency shift of the longitudinal FP modes whereas the differential gain is obtained by measuring the net modal gain from the FP modulation depth. The definition of α-factor in Eq. (1) is then equivalently expressed by:

$$\alpha = -\frac{2\pi}{L\delta\lambda}\frac{d\lambda/dI}{dG_{net}/dI} \tag{3}$$

where L is the cavity length, $\delta\lambda$ is the free spectral range while $d\lambda$ and dG_{net} are respectively the mode wavelength and net modal gain variations caused by the bias current change dI. However, it is important to stress that the main weakness of the ASE method results from its poor reliability if thermal effects are not properly eliminated. Indeed, thermal effects cause a red-shift of the optical wavelength and thereby interfere with the tracking of the carrier-induced blue-shift effect. In order to fully eliminate the thermal effects, a current source operated in the pulsed mode is highly preferred although it is also possible to use continuous-waves operation and eliminate the thermal effects by applying a correcting factor. Thus, the wavelength red-shift due to thermal effects, measured by varying the pump current right above threshold, is subtracted from the wavelength blue-shift measured below threshold. Following this protocol, the fitting error can certainly be minimized, however, the thermal correction holds under the assumption that thermal effects in QD lasers are unchanged below and above threshold as well as that the carriers are clamped above threshold. Nevertheless, the latter assumption is somewhat disputable for QD lasers, as the carrier population in resonant states keeps increasing with the bias currents, which will continue to enhance the gain and change the refractive index.

In what follows, the lasers under test are biased with a pulsed current using the shortest pulse width of 0.1 μs. The peak wavelength is then recorded by varying the duty cycle from 0.1% to 10 % with a step of 2 %. For each sub-threshold bias current, the peak wavelength values are plotted as a function of duty cycle and the extrapolation at 0 % duty cycle allows extracting the corresponding values without thermal effects. Figure 3(a) displays one peak wavelength measured for the

different sub-threshold currents ranging from 23.5 to 26.5 mA as a function of the duty cycle for the p-doped QD laser. By decreasing the duty cycle, the peak wavelength redshift is strongly attenuated due to the decrease of the thermal effects. Below 4% duty cycle the red-shift vanishes and the peak wavelength becomes blue-shifted. As such, by extrapolating down to 0% duty cycle (triangle markers), the extracted wavelengths corresponding to the limiting case for which thermal effects are gone. These values are then used for the determination of the α-factor. Figure 3(b) shows the peak wavelength

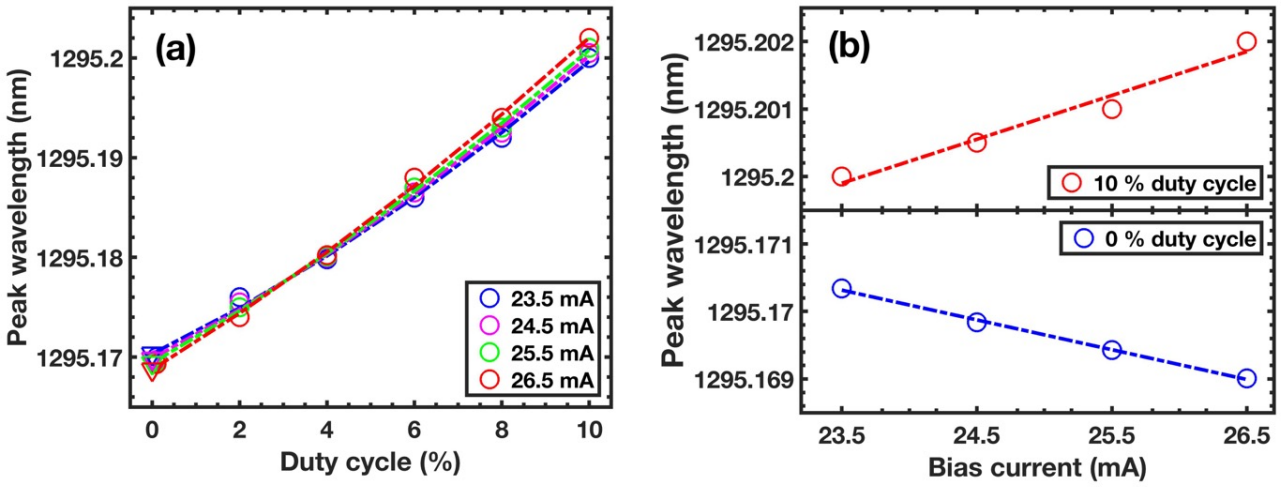

Figure 3. (a) Measured peak wavelength as a function of the duty cycle for different subthreshold bias currents. (b) Measured peak wavelength as a function of the bias current for two values of the duty cycle.

as a function of the bias currents for two duty cycles. The wavelength red-shift and blue-shift are clearly evidenced for the cases of 10% and 0% duty cycle. In addition, it is noted that the pulse width of 0.1 μs corresponds to the lower bound of the pulsewidth compared with a few microseconds usually used in many studies [15]. Besides, it is also important to stress that going below 0.1 μs would result in an extremely low output power and the impossibility to retrieve the gain and then the α-factor at the price of a poor accuracy. Therefore, a pulse width of 0.1 μs is typically what is recommended to almost eliminate all the thermal effects in the material. In order to investigate the influence of thermal effects on the α-factor, the

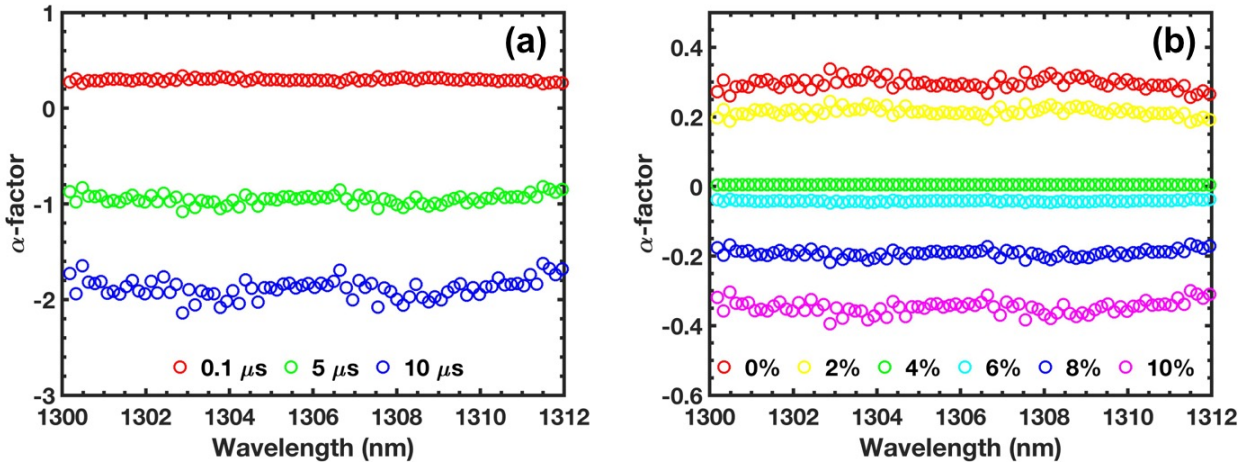

Figure 4. (a) Pulse width dependence of the measured α-factor at a fixed duty cycle of 0%. (b) Duty cycle dependence of the measured α-factor at a fixed pulse width of 0.1 μs.

pulse width dependence of the measured α-factor is also performed on a p-doped QD laser which has 3 QD layers and a 1.5 mm long cavity with a 3 μm wide ridge waveguide. As shown in figure 4(a), this laser has initial α-factor of about 0.3

which is found a bit larger than that of 5 QD laser due to the smaller material gain. However, when further increasing the pulse width from 0.1 μs to 5 μs and 10 μs, α-factor values extracted at a fixed duty cycle of 0 % are found reduced from 0.3 to negative values down to -1 at 5 μs and to -1.8 at 10 μs. This effect is attributed to the thermal effect induced wavelength red-shift below threshold which results in the negative α-factor values. Figures 4(b) also displays the measured α-factors extracted at a fixed pulse width of 0.1 μs as a function of different duty cycle ranging from 0 % to 10 % with a step of 2 %. The α-factors decrease from 0.3 to -0.35 along with the enhancement of the duty cycle from 0 % to 10 %. Therefore, the α-factors can be strongly underestimated if the thermal effects are not completed eliminated from the ASE method. In addition, the laser biased in the pulsed mode also resulting in a low signal-to-noise ratio and even irregular spectral line shape.

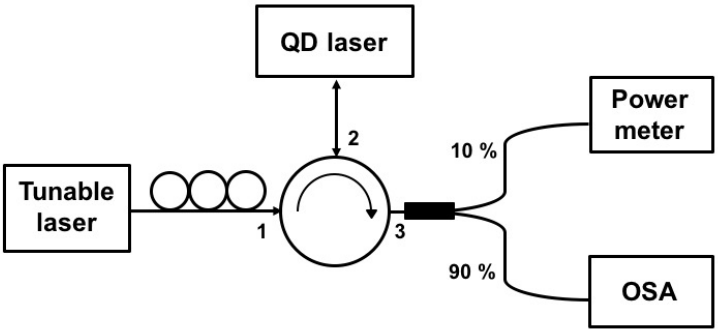

Figure 5. Experimental setup for measuring the α-factors.

Now, the α-factor is investigated with a thermally insensitive method using the residual side-mode dynamics under optical injection locking. Figure 5 illustrates the experimental setup where a tunable external cavity laser was used as the master laser and the injected light was coupled into the QD laser (slave laser) through an optical circulator. A polarization controller is inserted to align the polarization of both lasers. The 90 % of the output power was captured by a high resolution

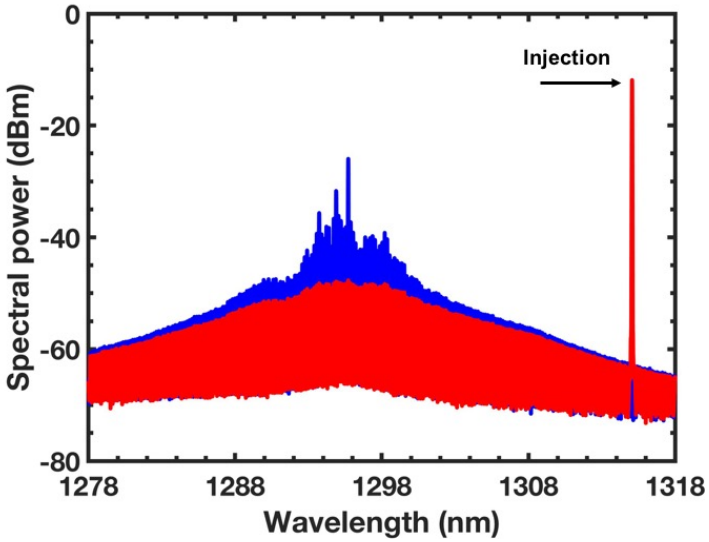

Figure 6. Measured optical spectra for the p-doped QD laser. The blue lines are for the free-running laser (i.e. without optical injection), and the red lines are for the laser is injection-locked.

optical spectrum analyzer (OSA) and the rest of 10 % was monitored by a power meter. The temperature of the slave laser was maintained at 20 ℃ throughout the experiment. The optical injection is performed far from the gain peak e.g. to a

longitudinal mode around 1315 nm, and the wavelength detuning is operated within the stable-locked regime. Owing to the gain reduction, the side modes are deeply suppressed in such way that the residual power of the side modes at the gain peak become governed by the ASE, and therefore the α-factor can be extracted as discussed hereinafter. Figure 6 illustrates the effect of optical injection on the FP cavity modes (blue lines) biased at 27.5 mA right above the threshold. Once the laser is stably-locked, only the mode subject to the optical injection keeps lasing (at 1315 nm) while all side modes are greatly suppressed (red lines). The frequency detuning (F_{inj}) is defined as the optical frequency difference between the master and slave lasers, while the injection ratio (R_{inj}) is the ratio of the injected signal power (P_{inj}) to the free-running slave laser power (P_0). Both the enhanced injection ratio and increased frequency detuning reduce the entire net modal gain compared to that of the free-running laser hence resulting in the suppression of the longitudinal side modes. The optical injection induced gain reduction can be understood through the corpuscular equations of the injection-locked oscillators, which under the steady-state conditions leads to the following expression [13]:

$$\Delta G_{net} = -\frac{2k_c}{v_g}\sqrt{R_{inj}P_o/P_s}\cos\varphi \tag{4}$$

where the phase φ of the laser field is given by:

$$\varphi = \sin^{-1}\left(-\frac{2\pi F_{inj}}{k_c\sqrt{R_{inj}P_0/P_S(1+\alpha^2)}}\right) - \tan^{-1}\alpha \tag{5}$$

with k_c is the coupling coefficient of the master laser to the slave laser, v_g is the light group velocity and P_S is the intra-cavity power of the slave laser under optical injection. The above equation shows that the F_{inj} reduces the net modal gain through the phase of the laser field. This gain reduction behavior is similar to that induced by the bias current in the ASE method. Therefore, the equation (3) can be re-expressed as follows:

$$\alpha = -\frac{2\pi}{L\delta\lambda}\frac{d\lambda/d\lambda_m}{dG_{net}/d\lambda_m} \tag{5}$$

with λ_m being the injection wavelength of the master laser. Consequently, an enhancement of the wavelength detuning shifts the lasing mode towards the longer wavelength side and reduces the gain to a lower level. Figure 7 describes the wavelength dependence of the net modal gain spectra for the p-doped QD laser. With the increase of the wavelength detuning, the whole gain spectra fall down gradually. Since this method is based on analyzing the residual side-mode ASE spectra under injection locking (IL), we named it ASE IL.

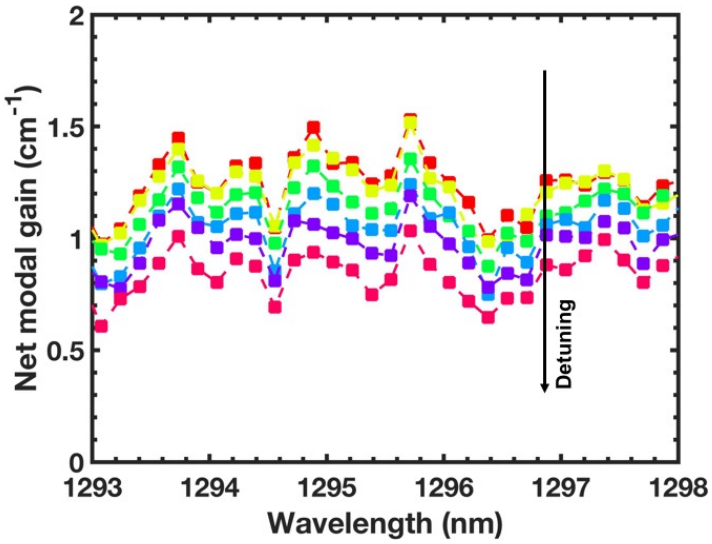

Figure 7. Wavelength variation of the measured net modal gain with detuning of the injected light from shorter to longer wavelength within the stable-locking range.

Figure 8 reveals the comparison of α-factors of the p-doped QD laser measured by ASE and ASE IL methods. In ASE IL method, the laser is biased at 27.5 mA just above the threshold current. The injected light is located at 1315 nm, which is 20 nm away from the gain peak of 1295 nm, while the R_{inj} is fixed at 5 dB. It is noted that this method is not sensitive neither to the injection power nor the choice of the injected mode due to the fact that the side modes are non-lasing and operated below threshold [13]. As shown in the Figure 8, the α-factors measured by ASE IL are found in a relatively good agreement with that measured under ASE and increase from about 0.14 at 1293 nm to 0.19 at 1299 nm, even though they are slightly higher. For example, compared with the α-factor of 0.13 at 1295 nm measured by ASE method, the α-factor measured by ASE IL is found with value of 0.15 with a standard deviation not exceeding 15%. This slight difference is attributed to the fact that ASE IL method relies on a fixed bias current while the ASE method requires a variation of the bias current hence leading to persistent device heating and underestimation of the α-factor. Therefore, the α-factor values measured under ASE IL are well consistent with the ASE values hence showing that this method is reliable and compatible with QD lasers onto silicon.

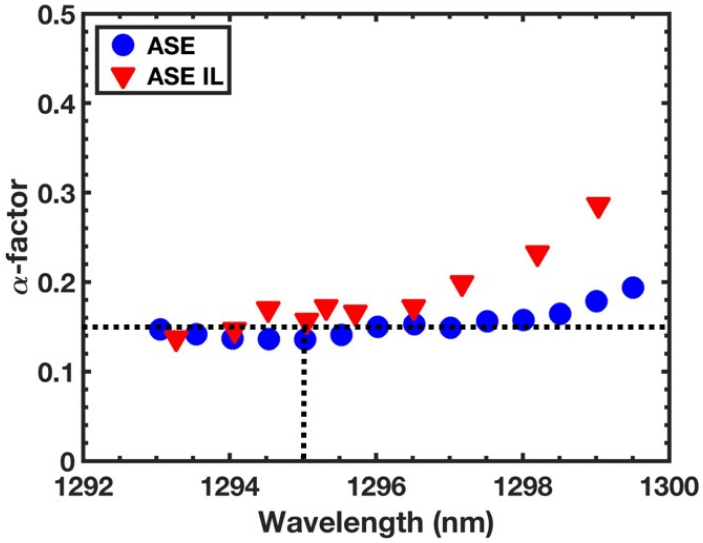

Figure 8. Wavelength dependence of the measured α-factor by ASE method and ASE IL method for p-doped QD laser. The horizontal dotted line indicates the gain peak α-factor value of 0.15, while the vertical dotted line indicates the position of FP gain peak.

4. CONCLUSIONS

To sum, this work investigates the extraction of the α-factors with a thermally insensitive method analyzing the residual side-mode dynamics under optical injection locking of QD lasers epitaxially grown onto silicon. The presented results perfectly confirm our initial measurements conducted with the standard ASE method i.e. the α-factor of the QD laser directly grown on silicon is very small and as low as 0.15 with a standard deviation not exceeding 15% which is very promising for the realization of integrated optical transmitters and increasing the maximum transmission distance in future silicon photonics systems.

ACKNOWLEDGMENTS

The authors acknowledge the financial support from ARPA-E (DE-AR000067) and the Institut Mines-Télécom.

REFERENCES

[1] Sun, C., et al, "Single-chip microprocessor that communicates directly using light," Nature, 528(7583), 534 (2015).
[2] Crowley, M. T., Naderi, N. A., Su, H., Grillot, F., Lester, L. F., and Bryce, A. C., "GaAs based quantum dot lasers," Advances in Semiconductor Lasers, 86(371), 42 (2012).

[3] Duan, J., Huang, H., Lu, Z., Poole, P., Wang, C., and Grillot, F., "Narrow spectral linewidth in InAs/InP quantum dot distributed feedback lasers," Appl. Phys. Lett., 112(12), 121102 (2018).
[4] Norman, J. C., Jung, D., Wan, Y., and Bowers, J. E., "Perspective: The future of quantum dot photonic integrated circuits," APL Photon., vol. 3, no. 3, p. 030901 (2018).
[5] Nishi, K., Takemasa, K., Sugawara, M., Arakawa, Y., "Development of Quantum Dot Lasers for DataCom and Silicon Photonics Applications," IEEE J. Sel. Top. Quantum Electron., vol. 23, no. 6, pp. 1-7 (2017).
[6] Otto, C., Globisch, B., Lüdge, K., Schöll, E. and Erneux, T., "Complex dynamics of semiconductor quantum dot lasers subject to delayed optical feedback," International J. Bifurcation & Chaos 22, 1250246 (2012).
[7] Huang, H., Duan, J., Jung, D., Liu, A. Y., Zhang, Z., Norman, J., Bowers, J. E., and Grillot, F., "Analysis of the optical feedback dynamics in InAs/GaAs quantum dot lasers directly grown on silicon," J. Opt. Soc. Am. B, 35(11), 2780-2787 (2018).
[8] Wieczorek, S., Krauskopf, B., Simpson, T. B. and Lenstra, D., "The dynamical complexity of optically injected semiconductor lasers," Phys. Rep., 416, 1-128 (2005).
[9] Huang, H., Schires, K., Poole, P. J., and Grillot, F., "Non-degenerate four-wave mixing in an optically injection-locked InAs/InP quantum dot Fabry-Perot laser," Appl. Phys. Lett., vol. 106, p. 143501(2015).
[10] Osinski, M. and Buus, J., "Linewidth broadening factor in semiconductor lasers - An overview," vol. 23, Issue 1, pp. 9-29 (1987).
[11] Koch, T. L. and Linke, R. A., "Effect of nonlinear gain reduction on semiconductor laser wavelength chirping," Appl. Phys. Lett., 48, 613 (1986).
[12] Duan, J., Huang, H., Jung, D., Zhang, Z., Norman, J., Bowers, J. E., and Grillot, F., "Semiconductor quantum dot lasers epitaxially grown on silicon with low linewidth enhancement factor," Appl. Phys. Lett., 112(25), 25111 (2018).
[13] Wang, C., Schires, K., Osiński, M., Poole, P. J., and Grillot, F., "Thermally insensitive determination of the linewidth broadening factor in nanostructured semiconductor lasers using optical injection locking," Sci. Rep., 6, 27825 (2016).
[14] Jung, D., Norman, J., Kennedy, M., Shang, C., Shin, B., Wan, Y., Gossard, A. C., and Bowers, J. E., "High efficiency low threshold current 1.3 μm InAs quantum dot lasers on on-axis (001) GaP/Si," Appl. Phys. Lett., 111(12), 122107 (2017).
[15] Tan, H., Mi, Z., Bhattacharya, P., and Klotzkin, D., "Dependence of Linewidth Enhancement Factor on Duty Cycle in InGaAs-GaAs Quantum-Dot Lasers," IEEE Photonics Technol. Lett., Vol. 20, No. 8 (2008).